

Detailed Garment Recovery from a Single-View Image

Shan Yang, Tanya Ambert, Zherong Pan, Ke Wang, Licheng Yu, Tamara Berg and Ming C. Lin
University of North Carolina at Chapel Hill

Most recent garment capturing techniques rely on acquiring multiple views of clothing, which may not always be readily available, especially in the case of pre-existing photographs from the web. As an alternative, we propose a method that is able to compute a rich and realistic 3D model of a human body and its outfits from a single photograph with little human interaction. Our algorithm is not only able to capture the global shape and geometry of the clothing, it can also extract small but important details of cloth, such as occluded wrinkles and folds. Unlike previous methods using full 3D information (i.e. depth, multi-view images, or sampled 3D geometry), our approach achieves detailed garment recovery from a single-view image by using statistical, geometric, and physical priors and a combination of parameter estimation, semantic parsing, shape recovery, and physics-based cloth simulation. We demonstrate the effectiveness of our algorithm by re-purposing the reconstructed garments for virtual try-on and garment transfer applications, as well as cloth animation for digital characters.

Categories and Subject Descriptors: I.3.7 [Computer Graphics]: Three-Dimensional Graphics and Realism—*Animation*; I.3.5 [Computer Graphics]: Computational Geometry and Object Modeling—*Physically based modeling*

General Terms: Experimentation, Human Factors

Additional Key Words and Phrases: Face animation, image-based modelling, iris animation, photorealism, physiologically-based modelling

ACM Reference Format:

Pamplona, V. F., Oliveira, M. M., and Baranoski, G. V. G. 2009. Photorealistic models for pupil light reflex and iridal pattern deformation. *ACM Trans. Graph.* 28, 4, Article 106 (August 2009), 11 pages.
DOI = 10.1145/1559755.1559763
<http://doi.acm.org/10.1145/1559755.1559763>

1. INTRODUCTION

Retail is a multi-trillion dollar business worldwide, with the global fashion industry valued at \$3 trillion [FashionUnited 2016]. Approximately \$1.6 trillion of retail purchasing was done via online e-commerce sales with growth rates in the double-digit [Lindner

2015]. Thus, enabling better online apparel shopping experiences has the potential for enormous economic impact. Given the worldwide demand for fashion and its obvious impact on the apparel industry, recent efforts toward technology-based solutions have been proposed, a few of which are already in use by commercial vendors. For example, there are several computer aided design (CAD) software systems developed specifically for the apparel industry. The apparel CAD industry has focused predominantly on sized cloth pattern development, pattern design CAD software, 3D draping preview, and automatic generation of 2D cloth patterns from 3D body scanners or other devices of measurements. Some of the leading apparel CAD companies include Gerber Technology, Lectra, Optitex, Assyst, StyleCAD, Marvelous Designer, Clo-3D, Avametric, etc. Unfortunately, these systems require careful and lengthy design by an apparel expert to develop.

More recently there have been efforts to develop virtual try-on systems, such as triMirror, that allow users to visualize what a garment might look like on themselves before purchasing. These methods enable 3D visualization of various garments, fast animation of dynamic cloth, and a quick preview of how the cloth drapes on avatars as they move around. However, the capabilities of these new systems in terms of ease-to-use and applicability are limited. Many of the virtual try-on systems use simple and fast image-based or texture-based techniques for a fixed number of avatar poses. They do not perform a complete simulation of how the fabric bends, wrinkles, or changes its physical appearance as a virtual human bends, stretches, or changes his/her pose in various activities. They also do not typically account for the effects due to the change of fabric materials under different conditions (e.g. changing weather, varying poses, weight fluctuation, etc). Furthermore, all of these virtual try-on systems assume either that the user selects one of a pre-defined set of avatars or that accurate measurements of their own bodies have been captured via 3D scans.

In this work, we consider the problem of recovering detailed models of garments from a single-view image. Such a capability enables users to virtually try on garments given only a single photograph of themselves wearing clothing. Instead of representing the clothed human as a single mesh [Chen et al. 2013; Li et al. 2012], we define a separate mesh for a person’s clothing, allowing us to model the rich physical interactions between clothing and the human body. This also helps capture highly occluded wrinkles in clothing that are caused by several sources, such as sewing patterns which incorporate pleats in garments, cloth material properties that influence the drape of the fabric, and the underlying human body pose and shape. Figure 1 illustrates some results generated by our system. In addition to virtual try-on applications, broader impacts in graphics include improving the accuracy of clothing models for animated characters, with the potential to further increase the visual realism of digital human models that already incorporate body-dependent priors for hair [Chai et al. 2012], face [Cao et al. 2013], skin [Nagano et al. 2015], and eyeballs [Bérard et al. 2014].

With limited input information from a single-view image, we constrain the problem solution space by exploiting three important priors. The first prior is a naked human body database that we use to construct a statistical human body model. This statistical model

Authors’ addresses: land and/or email addresses.

Permission to make digital or hard copies of part or all of this work for personal or classroom use is granted without fee provided that copies are not made or distributed for profit or commercial advantage and that copies show this notice on the first page or initial screen of a display along with the full citation. Copyrights for components of this work owned by others than ACM must be honored. Abstracting with credit is permitted. To copy otherwise, to republish, to post on servers, to redistribute to lists, or to use any component of this work in other works requires prior specific permission and/or a fee. Permissions may be requested from Publications Dept., ACM, Inc., 2 Penn Plaza, Suite 701, New York, NY 10121-0701 USA, fax +1 (212) 869-0481, or permissions@acm.org.

© 2009 ACM 0730-0301/2009/21-ART106 \$10.00

DOI 10.1145/1559755.1559763

<http://doi.acm.org/10.1145/1559755.1559763>

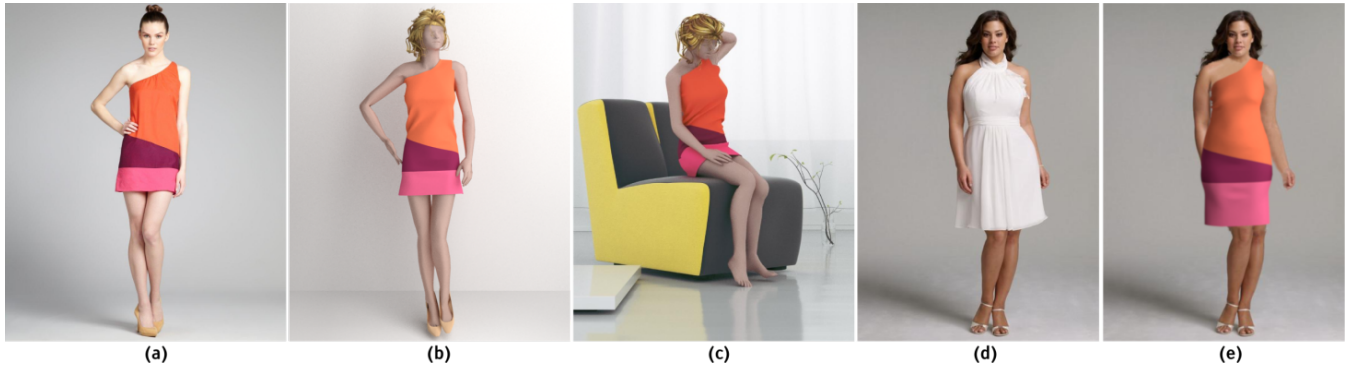


Fig. 1. **Garment recovery and re-purposing results.** From left to right, we show an example of (a) the original image [Saaclothes 2015] ©, (b) the recovered dress and body shape from a single-view image, and (c)-(e) the recovered garment dressed on another body of different poses and shapes/sizes [Hillsweddingdress 2015] ©.

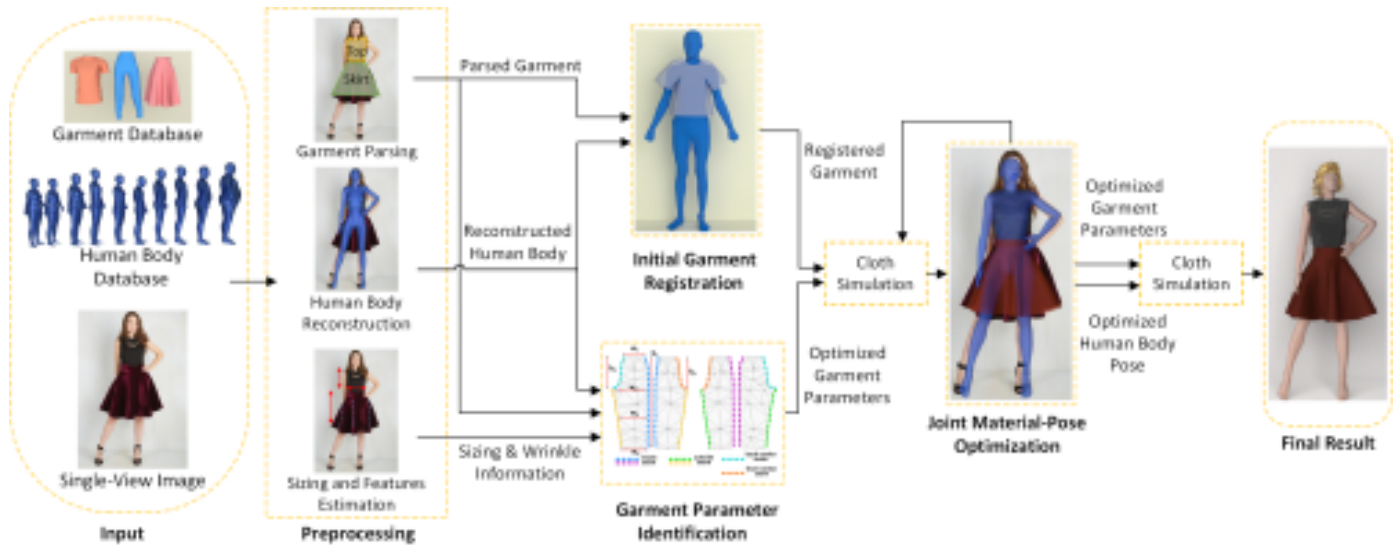


Fig. 2. **The flow chart of our algorithm.** We take a single-view image [ModCloth 2015] ©, a human-body dataset, and a garment-template database as input. We preprocess the input data by performing garment parsing, sizing and features estimation, and human-body reconstruction. Next, we recover an estimated garment described by the set of garment parameters, including fabric material, design pattern parameters, sizing and wrinkle density, as well as the registered garment dressed on the reconstructed body.

is used for extracting and matching the human body shape and pose in a given input image. The second prior is a database of garment templates for sewing patterns of various common garment types, such as skirts, pants, shorts, t-shirts, tank tops, and dresses. Finally, the third prior is the physically-based cloth simulation. Simulation helps provide additional 3D physical constraints lacking in a 2D image.

Our method proceeds as follows. To construct an accurate body model, the user indicates 14 joint positions on the image and provides a rough sketch outlining the human body silhouette. (This step can also be automated using image processing and body template for standard unoccluded poses.) From this information, we use a statistical human model to automatically generate a human body mesh for the image. To estimate the clothing model, we first compute a semantic parse of the garments in the image to identify and localize depicted clothing items. This semantic segmentation is computed automatically using a data-driven method for cloth-

ing recognition [Yamaguchi et al. 2013]. We then use the semantic parsing to extract garment sizing information such as waist girth, skirt length and so on, which are then used to map the depicted garments onto the existing garment templates and adjust the sewing patterns based on the extracted parameters. We also analyze the segmented garments to identify the location and density of wrinkles and folds in the recovered garments, which are necessary for estimating material properties of the garments.

Once we have obtained both the body and clothing models, we perform an image-guided parameter identification process, which optimizes the garment template parameters based on the reconstructed human body and image information. We then fit our 3D garment template’s surface mesh onto the human body to obtain the initial 3D garment, then jointly optimize the material parameters, the body shape and pose to obtain the final result. The flow chart of the overall process is shown in Fig. 2. Our main contributions include:

- An image-guided garment parameter selection method that makes the generation of virtual garments with diverse styles and sizes a simple and natural task (Section 5);
- A joint material-pose optimization framework that can reconstruct both body and cloth models with material properties from a single image (Section 6);
- Application to virtual try-on and character animation (Section 7).

2. RELATED WORK

Our work is built on previous efforts in cloth modeling, human pose/shape recovery, garment capture from single-view images, and semantic parsing.

Cloth Modeling: Cloth simulation is a traditional research problem in computer graphics. Early work on cloth simulation includes [Weil 1986; Ng and Grimsdale 1996; Baraff and Witkin 1998; House and Breen 2000]. More recently, a number of methods were proposed to solve the complicated problems presented in cloth simulation, including collision detection [Govindaraju et al. 2007; Tang et al. 2009; Curtis et al. 2008], collision handling, friction handling [Bridson et al. 2002], strain limiting [Goldenthal et al. 2007; English and Bridson 2008; Thomaszewski et al. 2009; Wang et al. 2010] and remeshing [Narain et al. 2012].

Realistic wrinkle simulation is an important problem in realistic cloth modeling. Volino and Magnenat-Thalmann [1999] introduced a geometric based wrinkle synthesis. Rohmer et al. [2010] presented a method to augment a coarse cloth mesh with wrinkles. Physically based cloth wrinkle simulation depends on the formulation of the cloth bending and stretching energy model. Different bending and stretching energy models [Bridson et al. 2003] were proposed for wrinkle simulation.

Garment modeling is built upon cloth simulation. It also needs to take the design and sewing pattern of the garment into consideration. Some methods start from the 2D design pattern [Protosaltou et al. 2002; Decaudin et al. 2006; Berthouzoz et al. 2013] or 2D sketches [Turquin et al. 2007; Robson et al. 2011]. Other methods explore garment resizing and transfer from 3D template garments [Wang et al. 2005; Meng et al. 2012; Sumner and Popović 2004]. Our work synthesizes different ideas and extends these methods to process 2D input image and fluidly transfer the results to simulation of 3D garments. We edit the 2D sewing patterns with information extracted from a single-view image, which is then used to guide the generation of garments of various sizes and styles.

Human Pose and Shape Recovering: Human pose and shape recovery from a single-view image is extensively studied in computer vision and computer graphics. Taylor [2000] presented an articulated-body skeleton recovery algorithm from a single-view image with limited user input. Agarwal et al. [2006] proposed a learning-based method to recover the human body pose from monocular images. We refer readers to this survey on human motion recovery and analysis [Moeslund et al. 2006].

Human pose and shape recovery in computer graphics focuses more on reconstructing muscle accurately and watertight 3D human body meshes. For character animation, a realistic 3D human body mesh is the basis. To recover clothing with rich details, a human body mesh is required. For human body mesh generation, we follow the previous data-driven methods, most of which are PCA based. These techniques use a set of bases to generate a variety of human bodies of different poses and shapes. Seo and Thalmann [2003] presented a method to construct human body meshes of different shapes. Following this work, Anguelov et al. [2005] posed the SCAPE model that can produce human body meshes of different poses and shapes. Hasler et al. [2009] encode both human

body shapes and poses using PCA and semantic parameters. Built upon these previous models, Zhou et al. [2010] proposed a method to recover the human body pose and shape from a single-view image.

Clothing Capturing: In the last decade, many methods have been proposed for capturing clothing from images or videos. Methods can be divided into two categories: marker-based and markerless. Most marker-based clothing capture methods require the markers to have been printed on the surface of the cloth. Different kinds of markers were used for the capture [Scholz and Magnor 2006; Hasler et al. 2006; Tanie et al. 2005; Scholz et al. 2005]. Furthermore, markerless methods can be characterized into single-view [Zhou et al. 2013], depth camera based [Chen et al. 2015] and multi-view methods [Popa et al. 2009]. The primary limitations of these methods include the lack of garment details and material properties, the loss of the original garment design, and the complexity of the capturing process. In contrast, our method can retrieve the 2D design pattern with the individual measurements obtained directly from a single image. With the joint human pose and clothing optimization method, our algorithm recovers realistic garment models with details (e.g. wrinkles and folds) and material properties.

Semantic Parsing: Semantic parsing is a well studied problem in computer vision, where the goal is to assign a semantic label to every pixel in an image. Most prior work has focused on parsing general scene images, e.g. [Long et al. 2015; Farabet et al. 2013; Pinheiro and Collobert 2014]. We work on the somewhat more constrained problem of parsing clothing in an image. To obtain a semantic parse of the clothing depicted in an image, we make use of the data-driven approach by Yamaguchi et al. [2013]. This method automatically estimates the human body pose from a 2D image, extracts a visual representation of the clothing the person is wearing, and then visually matches the outfit to a large database of clothing items to compute a cloth parsing for the query image.

3. PROBLEM STATEMENT AND ASSUMPTIONS

In this section, we give the formal definition of the problem. The input to our system is an RGB image Ω . We assume the image is comprised of three parts: the background region Ω_b , the foreground naked human body parts Ω_h and the foreground cloth Ω_c , where $\Omega = \Omega_b \cup \Omega_h \cup \Omega_c$. In addition, we assume that both the human body and the cloth are in a statically stable physical state. Although this assumption precludes images capturing a fast moving human, it provides a crucial assumption for our joint optimization algorithm.

Our goal is to simultaneously recover the garment described by a set of parameters $\langle \mathcal{C}, \mathcal{G}, \mathbf{U}, \mathbf{V} \rangle$, along with a set of parameters $\langle \theta, \mathbf{z} \rangle$ that encode human body pose and shape obtained from the image, and a set of parameters $\langle \mathcal{L}, \mathcal{P} \rangle$ defining the 2D sizing parameters and wrinkle density of the reference garment. For the clothing parameters, \mathcal{C} is the set of material parameters including stretching stiffness and bending stiffness coefficients, \mathbf{U} is the 2D triangle mesh representing the garment's pattern pieces, and \mathbf{V} is the 3D triangle mesh representation of the garment. For each triangle of the 3D garment mesh \mathbf{V} , there is a corresponding one in the 2D space of \mathbf{U} . For each mesh vertex $\mathbf{x}_i \in \mathbf{V}$, such as those lying on a stitching seam in the garment, there might be multiple corresponding 2D vertices $\mathbf{u}_i \in \mathbf{U}$. The parameter \mathcal{G} is the set of parameters that defines the dimensions of the 2D pattern pieces. For example, we define the parameter $\mathcal{G}_{\text{pants}} = \langle w_1, w_2, w_3, w_4, h_1, h_2, h_3 \rangle$ for pants, where the first four parameters define the waist, bottom, knee and ankle girth and the last three parameters indicate the total length, back upper,

and front upper length. For each basic garment category, we can manually define this set of parameters \mathcal{G} . By manipulating the values of the parameters \mathcal{G} , garments of different styles and sizes can be modeled, e.g. capri pants vs full-length pants, or tight-fitting vs loose and flowy silhouettes.

For the human-body parameters, θ is the set of joint angles that together form the body pose, and \mathbf{z} is the set of semantic parameters that describe the body shape. We follow the PCA encoding of the human body shape presented in [Hasler et al. 2009]. The semantic parameters include gender, height, weight, muscle percentage, breast girth, waist girth, hip girth, thigh girth, calf girth, shoulder height and leg length. Table 3 provides a list of formal definitions for the notation used in this paper.

Table I. **Notation and definition of our method.**

NOTATION	DEFINITION
\mathcal{C}	material property parameters of the garment
\mathcal{G}	garment parameters
$\mathcal{G}_{\text{pants}}$	$\langle w_1, w_2, w_3, w_4, h_1, h_2, h_3 \rangle$
$\mathcal{G}_{\text{skirt}}$	$\langle l_1, r_1, r_2, \alpha \rangle$
\mathcal{G}_{top}	$\langle r, w_1, w_2, h_1, h_2, l_1 \rangle$
\mathbf{U}	2D triangle mesh representing garment pattern
\mathbf{u}_i	vertex of the 2D garment pattern mesh
\mathbf{V}	3D triangle surface mesh of the garment
\mathbf{x}_i	vertex of the 3D triangle mesh
\mathcal{L}	pixel-wise sizing parameters of the 2D segmented garment in the image
\mathcal{P}	wrinkle edges of the 2D segmented garment in the image
\mathbf{k}	bending stiffness parameters
\mathbf{w}	stretching stiffness parameters
\mathbf{F}	deformation gradient of the deforming garment
\mathcal{K}	garment 3D mesh curvature measurement
\mathcal{S}	garment 3D mesh sizing measurement
Ψ	bending energy of the garment
Φ	stretching energy of the garment
$v_{i,j}$	rigging weights of the 3D garment mesh
β	joint angles of the skeleton of the 3D garment mesh
θ	joint angles of the human body mesh
\mathbf{z}	semantic parameters of the human body mesh shape
\mathbf{p}_i	vertex of the 3D human body mesh
\mathbf{Z}_i	PCA basis of human body shape
ω_i	rigging weights of the human body mesh
\mathcal{D}_c	garment database
\mathcal{D}_h	human body database

4. DATA PREPARATION

This section describes the data preprocessing step. We begin with the data representations for the garment and the human body, followed by a brief description of each preprocessing module.

4.1 Data Representations

The garment template database can be represented as a set $\mathcal{D}_c = \{ \langle \mathcal{C}_i, \mathcal{G}_i, \mathbf{U}_i, \mathbf{V}_i \rangle \mid i \in 1, \dots, N \}$, where N is the number of garment templates. Each garment template consists of a 2D triangle mesh \mathbf{U} representing the sewing pattern, a 3D mesh \mathbf{V} , a set of dimension parameters \mathcal{G} for each pattern piece, and a set of material parameters \mathcal{C} . The human body template database $\mathcal{D}_h = \{ \langle \theta_j, \mathbf{z}_j \rangle \mid j \in 1, \dots, M \}$ consists of M naked human body meshes with point to point correspondence. We use several human body datasets, including the SCAPE dataset [Angelov

et al. 2005], the SPRING dataset [Yang et al. 2014], the TOSCA dataset [Bronstein et al. 2008; Young et al. 2007; Bronstein et al. 2006], and the dataset from [Hasler et al. 2009].

Parameterized Human Model: Given the body database \mathcal{D}_h , we extract a statistical shape model for human bodies. Under this model, each world space vertex position \mathbf{p}_i on the human body is parameterized as:

$$\mathbf{p}_i(\theta, \mathbf{z}) = \sum_i \omega_i \mathcal{T}_{\mathcal{B}_i}(\theta) (\mathbf{p}_i^0 + \mathbf{Z}_i \mathbf{z}), \quad (1)$$

which is a composition of a linear blend skinning model [Kavan et al. 2010] and an active shape model [Zhao et al. 2003]. Here ω_i and \mathcal{B}_i are the set of weights and bones associated with the vertex i . $\mathcal{T}_{\mathcal{B}_i}$ is the transformation matrix of bone \mathcal{B}_i . \mathbf{p}_i^0 and \mathbf{Z}_i are the mean shape and active shape basis at the rest pose, respectively. The basis \mathbf{Z}_i is calculated by running PCA [Hasler et al. 2009] on \mathcal{D}_h .

4.2 Preprocessing

Our preprocessing step consists of: a) human body reconstruction to recover the human body shape and pose from the input image, b) garment parsing to estimate the locations and types of garments depicted in the image, and c) parameter estimation to compute the sizing and fine features of the parsed garments.

Human Body Reconstruction: Our human body recovery relies on limited user input. The user helps us identify the 14 human body joints and the human body silhouette. With the identified joints, a human body skeleton is recovered using the method presented in [Taylor 2000]. The recovery of the human body shape is done by optimizing the semantic parameters \mathbf{z} to match the silhouette. In this step, we ignore the camera scaling factor.

Garment Parsing: We provide two options for garment parsing. The first uses the automatic computer vision technique presented in [Yamaguchi et al. 2013]. This approach combines global pre-trained parse models, local models learned from nearest neighbors, and transferred parse masks to estimate the types of garments and their locations on the person. The second option requires assistance from the user. Given the image Ω we extract the clothing regions $\Omega_{b,h,c}$ by performing a two stage image segmentation guided by user sketch. In the first stage, a coarse region boundary is extracted using a graph cut algorithm [Li et al. 2004]. Then, the region is refined via re-clustering [Levin et al. 2008].

Sizing and Features Estimation: Given the pixel level segmentation of the garment, the next step is to estimate the garment information $\langle \mathcal{L}, \mathcal{P} \rangle$ from the image. The garment sizing parameters \mathcal{L} are computed from the pixel level garment segmentation. We extract fine features, such as fold and wrinkle edges \mathcal{P} , from the garment images using the technique described in [Popa et al. 2009]. We first detect edges using Holistically-Nested edge detection [Xie and Tu 2015], and then smooth the edges by fitting them to low-curvature quadrics. We smooth edges split during the detection phase by merging those that have nearby endpoints and similar orientations. Finally, we form 2D folds by matching parallel edges. This pairing favors long edges with bright regions in between. Edges not part of a pair are unlikely to contribute to a fold, and are discarded.

4.3 Initial Garment Registration

Our initial clothing registration step aims to dress our template garment onto a human body mesh of any pose or shape. We optimize the vertex positions of the 3D mesh, \mathbf{x} , of the template clothing

based on the human body mesh parameters $\langle \theta, \mathbf{z} \rangle$. In this step, we ignore the fit of the clothing on the human body (fixing the triangle mesh \mathbf{U} in this step). We follow the method proposed in [Brouet et al. 2012] for registering a template garment to a human body mesh with a different shape. However, their method is unable to fit the clothing to human meshes with varying poses; we extend their approach by adding two additional steps.

The first step requires the alignment of the joints \mathcal{Q}_c of the template garment skeleton with the joints \mathcal{Q}_h of the human body mesh skeleton, as shown in Fig. 3. Each joint $\mathbf{q} \in \mathcal{Q}_c$ of the garment has one corresponding joint $\mathbf{t} \in \mathcal{Q}_h$ of the human body mesh. We denote the number of joints of the garment as K_c . This step is done by applying a rigid body transformation matrix \mathbf{T} on the joint of the garment.

$$E_{\text{joints}} = \underset{\mathbf{T}}{\operatorname{argmin}} \sum_{i=0, \mathbf{q}_i \in \mathcal{Q}_c, \mathbf{t}_i \in \mathcal{Q}_h}^{K_c} \|\mathbf{T}\mathbf{q}_i - \mathbf{t}_i\| \quad (2)$$

Next, we need to fit this transformed 3D template garment mesh onto the human body mesh with pose described by parameter θ , the vector of the angles of the joints. Our template garment is then deformed according to θ . We denote the vector β as the joint angles of the template garment mesh. We set the value of the vector β_i to the value of the corresponding joint angle θ_i of the human body mesh. Then, we compute the 3D garment template mesh to match the pose of the underlying human body mesh according to this set of joint angles β by,

$$\mathbf{x}_i(\beta) = \sum_j v_{ij} \mathcal{T}_{\mathcal{B}_j}(\beta) \mathbf{x}^0, \quad (3)$$

where v_{ij} is the weights of bone \mathcal{B}_j on vertex \mathbf{x}_i and $\mathcal{T}_{\mathcal{B}_j}$ is the transformation matrix of the bone \mathcal{B}_j . An example result is shown in Fig. 3c.

The final step is to remove collisions between the garment surface mesh and the human body mesh. This step is similar to the ICP algorithm proposed by Hao Li et al. [2008]. We introduce two constraints: rigidity and non-interception. The deformation of the clothing should be as rigid as possible. After this step, we have an initial registered garment with a 3D mesh $\hat{\mathbf{V}}$ that matches the underlying human pose and is free of interpenetrations with the human body. We show the our initial garment registration results in Fig. 4.

5. IMAGE-GUIDED PARAMETER IDENTIFICATION

Starting from our 2D triangle mesh \mathbf{U} of the pattern pieces, we select garment parameters based on the sizing and fine-detail parameters $\langle \mathcal{L}, \mathcal{P} \rangle$ estimated from the source image. In this step, we adjust $\langle \mathcal{C}, \mathcal{G}, \mathbf{U} \rangle$ but fix the 3D mesh $\hat{\mathbf{V}}$ to obtain the garment that best matches the one shown in the image. Specific information we need from the image are the sizing information \mathcal{L} and wrinkle edges \mathcal{P} of the clothing. For example, for a skirt, we need to estimate the waist girth and the length of the skirt from the image. Using this information we initialize the parameter \mathcal{G} . The wrinkle density, derived from the wrinkle edges \mathcal{P} of the skirt provides important hints about material properties, such as stretching and bending. Based on the wrinkle information computed from the image, we optimize both the fabric material parameters \mathcal{C} and the adjusted dimensions of the garment pattern \mathcal{G} .

For basic garments types, such as skirt, pants, t-shirts, and tank tops, we use one template pattern for each. We modify the classic sewing pattern according to the parameters \mathcal{G} . By adjusting

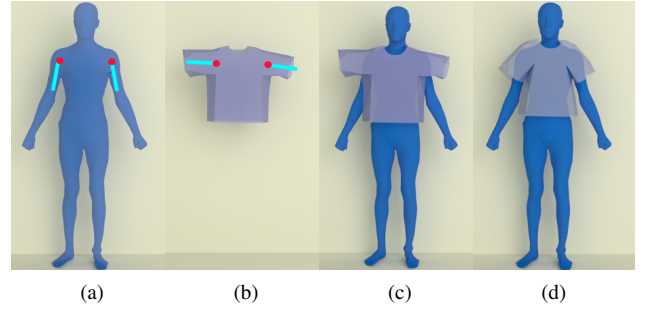


Fig. 3. **Initial garment registration process.** (a) The human body mesh with the skeleton joint shown as the red sphere and the skeleton of the arm shown as the cyan cylinder. (b) The initial t-shirt with the skeleton joint shown as the red sphere and the skeleton of the sleeve part of it shown as the cyan cylinder. (c) The t-shirt and the human body mesh are aligned by matching the joints. (d) The result after aligning the skeleton and removing the interpenetrations.



Fig. 4. **Initial garment registration results.** We fit a garment to human bodies with different body shapes and poses.

the garment parameters \mathcal{G} and fabric material parameters \mathcal{C} , we recover basic garments of different styles and sizes. The classic circle skirt sewing pattern is shown in Fig. 5a. Our parametric space, which is morphed from this circle sewing pattern, is shown in Fig. 5b. For the skirt pattern, there are four parameters to optimize $\mathcal{G}_{\text{skirt}} = \langle l_1, r_1, r_2, \alpha \rangle$. The ratio between the parameter l_1 and r_2 is constrained by the waist girth and skirt length information extracted from the image. The other two parameters r_1 and α are constrained by the wrinkle density. With different garment parameters, skirts can vary from long to short, stiff to soft, and can incorporate more or fewer pleats, enabling us to model a wide variety of skirts from a single design template.

Similarly for pants, the classic sewing pattern and our template pattern pieces are shown in Fig. 5c and Fig. 5d. There are seven parameters for the dimensions of the pants template $\mathcal{G}_{\text{pants}} = \langle w_1, w_2, w_3, w_4, h_1, h_2, h_3 \rangle$ with the first four parameters describing the waist, bottom, knee and ankle girth and the last three parameters representing the total length, back-upper and front-upper length. The t-shirt sewing pattern is shown in Fig. 5e and our parametric t-shirt pattern is shown in Fig. 5f with the garment parameters $\mathcal{G}_{\text{tshirt}} = \langle r, w_1, w_2, h_1, h_2, l_1 \rangle$. Among the parameters $\mathcal{G}_{\text{tshirt}}$, parameter r describes the neckline radius, w_1 describes the sleeve width, w_2 describes the shoulder width, h_1 describes the bottom length, h_2 describes the total length, and l_1 describes the length of the sleeve.

Many wrinkle patterns of garments, especially in skirts and dresses, are formed due to the sewing patterns. Different sewing patterns result in very different garments. Traditional sewing techniques form skirt wrinkles by cutting the circular portion of the pattern. To simulate this process but make it generally applicable, we

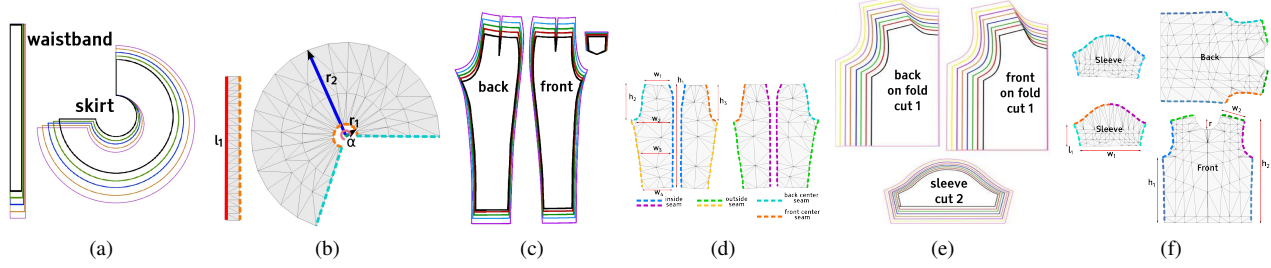


Fig. 5. **Template sewing pattern and parameter space of a skirt, pants, and t-shirt.** (a) The classic circle sewing pattern of a skirt. (b) Our parametric skirt template showing dashed lines for seams and the four parameters $\langle l_1, r_1, r_2, \alpha \rangle$, in which parameter l_1 is related to the waist girth and parameter r_2 is related to the length of the skirt. (c) The classic pants sewing pattern. (d) Our parametric pants template with seven parameters $\langle w_1, w_2, w_3, w_4, h_1, h_2, h_3 \rangle$. (e) The classic t-shirt sewing pattern. (f) Our parametric t-shirt template with six parameters $\langle r, w_1, w_2, h_1, h_2, l_1 \rangle$.

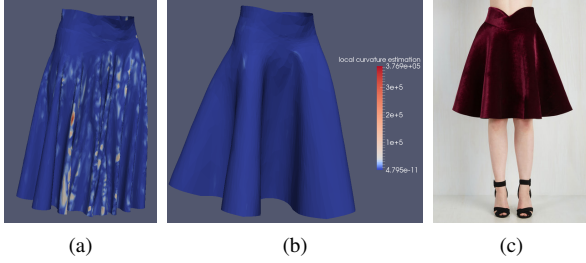


Fig. 6. **Material parameter identification results.** (a) The local curvature estimation before optimizing the bending stiffness coefficients (using the cool-to-hot color map). (b) The local curvature estimation after the optimization. (c) The original garment image [ModCloth 2015] ©. modify the parameter \mathcal{G} to achieve the same effect. Besides sewing pattern, professional garment designers take advantage of cloth material properties as well to produce different styles of clothing. We tune the bending stiffness coefficients and stretching stiffness coefficients in \mathcal{C} to simulate this cloth selection process.

We match the wrinkle density identified in the image by minimizing the local curvature differences between our recovered garment $\mathcal{K}(\mathcal{C}, \mathcal{G})$ and the reference garment $\mathcal{K}(\mathcal{P})_{\text{target}}$ in the single-view image. The reference garment local curvature $\mathcal{K}(\mathcal{P})_{\text{target}}$ is computed by projecting the image information onto our 2D garment pattern pieces \mathbf{U} . The projection process includes two steps: estimation and linear interpolation. We first approximate the local curvature threshold for the sharp wrinkles and smooth folds. The local curvature threshold for one sharp wrinkle is up to 10^5 m^{-1} and that for smooth folds is close to 10^{-4} m^{-1} . Sharp wrinkles or large folds are determined by the density of the extracted 2D wrinkles. The projection process (with the projection matrix \mathcal{H}) is,

$$\mathcal{K}(\mathcal{P})_{\text{target}} = \mathcal{H}\mathcal{P}. \quad (4)$$

The sizing and style of the garment described by the parameter \mathcal{L} obtained from the parsed garment are matched by minimizing the sizing differences between our recovered garment $\mathcal{S}(\mathcal{C}, \mathcal{G})$ and the reference garment projected onto the recovered human body mesh $\mathcal{S}(\mathcal{L}, \mathbf{z})_{\text{target}}$. The projection matrix \mathbf{H} maps \mathcal{L} of the 2D image Ω to the 3D human body mesh $\langle \theta, \mathbf{z} \rangle$. The values on the diagonal depend on the semantic parameters \mathbf{z} which describe the shape of the underlying human body. The projection is expressed as,

$$\mathcal{S}(\mathcal{L}, \mathbf{z})_{\text{target}} = \mathbf{H}(\mathbf{z})\mathcal{L}. \quad (5)$$

We ignore the camera scaling factor in this step since the input is a single-view image. It is natural to scale the recovered clothing and human body shape as a post processing step.

Combining these two objectives, our optimization process can be formulated as,

$$\mathbf{E}_{\text{mat}} = \underset{\mathcal{C}, \mathcal{G}}{\text{argmin}} \|\mathcal{K}(\mathcal{C}, \mathcal{G}) - \mathcal{K}(\mathcal{P})_{\text{target}}\| + \|\mathcal{S}(\mathcal{C}, \mathcal{G}) - \mathcal{S}(\mathcal{L}, \mathbf{z})_{\text{target}}\|. \quad (6)$$

Local curvature κ estimation at each vertex is computed based on the bending between the two neighboring triangles sharing the same edge. For each vertex \mathbf{x} of the two triangles that share an edge \mathbf{e} , the local curvature κ is computed following the approach from Wang et al. [2011] and Bridson et al. [2003],

$$\kappa = \|\sin(\alpha/2)(h_1 + h_2)^{-1}|\mathbf{e}|\mathbf{x}\|, \quad (7)$$

where h_1 and h_2 are the heights of the two triangles that share the edge \mathbf{e} and α is the supplementary angle to the dihedral angle between the two triangles. The corresponding bending force \mathbf{f}_{bend} for each vertex \mathbf{x} is computed as,

$$\mathbf{f}_{\text{bend}} = k \sin(\alpha/2)(h_1 + h_2)^{-1}|\mathbf{e}|\mathbf{x}, \quad (8)$$

where k is the bending stiffness coefficient.

Stretching also affects the formation of wrinkles. Each triangle $\langle \mathbf{u}_0, \mathbf{u}_1, \mathbf{u}_2 \rangle$ in the 2D template mesh is represented as $D_m = \begin{bmatrix} \mathbf{u}_1 - \mathbf{u}_0 \\ \mathbf{u}_2 - \mathbf{u}_0 \end{bmatrix}$, and each triangle in the 3D garment mesh $\langle \mathbf{x}_0, \mathbf{x}_1, \mathbf{x}_2 \rangle$ is represented as $d_m = \begin{bmatrix} \mathbf{x}_1 - \mathbf{x}_0 \\ \mathbf{x}_2 - \mathbf{x}_0 \end{bmatrix}$. The stretching forces $\mathbf{f}_{\text{stretch}}$ are computed by differentiating the stretching energy Ψ which depends on the stretching stiffness parameter \mathbf{w} , the deformation gradient $\mathbf{F} = d_m D_m^{-1}$ and the Green strain tensor $\mathbf{G} = \frac{1}{2}(\mathbf{F}^T \mathbf{F} - \mathbf{I})$ against the vertex 3D position \mathbf{x} ,

$$\mathbf{f}_{\text{stretch}} = \frac{\partial \Psi(\mathbf{w}, \mathbf{F})}{\partial \mathbf{x}}. \quad (9)$$

Before we start the optimization of Eqn. 6, we constrain the parameter space. We use the ‘‘Gray Interlock’’ presented in [Wang et al. 2011], which is composed of 60% cotton and 40% polyester as the ‘‘softest’’ material, meaning it bends the easiest. We multiply the bending parameters of this material by 10^2 to give the ‘‘stiffest’’ material. Our solution space is constrained by these two materials and we initialize our optimization with the ‘‘softest’’ material parameters.

The optimization is an iterative process, alternating between updates for parameters \mathcal{G} and \mathcal{C} . We found the value of the objective function is more sensitive to the cloth material properties \mathcal{C} than to the parameter \mathcal{G} , so we maximize the iterations when optimizing for \mathcal{C} , fixing \mathcal{G} . The optimization of parameter \mathcal{C} is coupled with the cloth dynamics. We drape the initial fitted garment onto the human body mesh. The garment is in the dynamic state and subject

to gravity. The physically based draping operation is an optimization process. When the bending energy $\Phi(\mathbf{k}, \kappa)$ and the stretching energy $\Psi(\mathbf{w}, \mathbf{F})$ are minimized, the clothing is in the rest state. We couple our parameter estimation with this physically based simulation process. During the simulation, we change the cloth material parameters \mathcal{C} so that the local curvature κ matches the targeting threshold $\mathcal{K}_{\text{target}}$. That is to say, when the simulator minimizes the energy Φ , our optimizer minimizes $\|\mathcal{K} - \mathcal{K}_{\text{target}}\|$ by changing the bending stiffness parameters \mathbf{k} and stretching stiffness parameters \mathbf{w} . We apply the L-BFGS [Liu and Nocedal 1989] method for our material parameter optimization. When the clothing reaches a static state, the optimizer switches to optimizing parameter \mathcal{G} . The optimizer for the parameter \mathcal{G} is not coupled with the garment simulation. The objective function is evaluated when the clothing reaches the static state. We adopt the Particle Swarm Optimization method [Kennedy 2010] for the parameter \mathcal{G} optimization. We use 40 particles for the parameter estimation process. The alternating process usually converges after four steps. One example result of the garment parameter process is shown in Fig. 6.

6. JOINT MATERIAL-POSE OPTIMIZATION

6.1 Optimal Parameter Selection

The parameter identification step provides us with the initial recovered garment described by the set of parameters $\langle \mathcal{C}', \mathcal{G}', \mathbf{U}' \rangle$. Many realistic garment wrinkles and folds, however, are formed due to the underlying pose of the human body. Therefore, in this step, we further refine our results by optimizing both the pose parameters of the human body θ and the material properties of the cloth \mathcal{C}' . The optimization objective for this step is,

$$\mathbf{E}_{\text{joint}} = \operatorname{argmin} \|\mathcal{K}(\mathcal{C}, \theta) - \mathcal{K}(\mathcal{P})_{\text{target}}\|. \quad (10)$$

The optimization process is similar to the garment parameter identification step, alternating between updating the pose parameter θ and the material parameters \mathcal{C}' . The objective function (Eqn. 10) is more sensitive to the pose parameter θ than to the material parameters \mathcal{C}' . We constrain the optimization space of parameter θ by confining the rotation axis to only the three primal axes. An example of our joint material-pose optimization method is shown in Fig. 7.



Fig. 7. **Joint Material-Pose Optimization results.** (a) The pants recovered prior to the joint optimization. (b) The recovered pants after optimizing both the pose and the material properties. The wrinkles in the knee area better match with those in the original image. (c) The original pants image [Anthropologie 2015] ©.

6.2 Application to Image-Based Virtual Try-On

This joint material-pose optimization method can be applied directly to image-based virtual try-on. We first recover the shape and pose of the human body $\langle \theta, \mathbf{z} \rangle$ from the single-view image. Then, we dress the recovered human body with the reconstructed

garments $\langle \tilde{\mathcal{C}}, \tilde{\mathcal{G}}, \tilde{\mathbf{U}}, \hat{\mathbf{V}} \rangle$ from other images. We perform the initial garment registration step (Sec. 4.3) to fit the 3D surface mesh $\hat{\mathbf{V}}$ onto the recovered human body $\langle \theta, \mathbf{z} \rangle$.

Existing state-of-the-art virtual try-on rooms require a depth camera for tracking, then overlay the human body with the fitting garment. Our algorithm, on the other hand, is able to fit the human body from a single 2D image with an optimized virtual outfit recovered from other images. We provide the optimized design pattern together with a 3D view of the garment fitted to the human body.

The fitting step requires iterative optimization in both the garment parameters and the human-body poses. As in a real fitting process, for human bodies with different sizes and shapes, we vary the sizing of the outfits accordingly. When editing in parameter space using the methods introduced in the previous section, we ensure that the outfit can fit on the human body without distorting the original design. For each basic garment we use one template pattern and the corresponding set of parameters. To preserve the garment design, we do not change the material properties of the fabric when virtually fitting the garment to a new mannequin.

7. RESULTS AND DISCUSSION

We have implemented our algorithm in C++ and demonstrated the effectiveness of our approach throughout the paper. In this section, we show example results, performance, and comparisons to other garment recovery methods.

Garment Recovery from a Single-view Image: We show several examples of garment recovery from a single-view image. In Fig. 8 and Fig. 9, we show our method can recover garments of different styles and materials. Fig. 10 demonstrates the effectiveness of our method for the recovery of highly occluded garments. It also shows our recovered garment can be applied to human bodies in different poses.

Image-Based Garment Virtual Try-On: We show examples of our image-based garment virtual try-on method (Sec. 6.2) in Fig. 1 and Fig. 11. We can effectively render new outfits onto people from only a single input image.

Evaluation: We evaluate the accuracy of the recovered sizing parameters \mathcal{G} and local curvature \mathcal{K} using synthetic scenes. Each synthetic scene has two lighting conditions, mid-day and sunset (shown in Fig. 12). We fix the both the extrinsic and the intrinsic camera parameters for scene rendering, and the garments are in static equilibrium. Through the ten test cases, we aim to validate the accuracy and reliability of our method against different human poses, and lighting conditions. The evaluation result is shown in Table II and Table III after eliminating the camera scaling factor. We found that the lighting condition mainly affects the body silhouette approximation, and the garment folding parsing. And the pose affects the body skeleton approximation. Overall, we achieve higher than **83%** accuracy for recovering the sizing parameters \mathcal{G} under different human poses and lighting conditions. We evaluate the accuracy of the recovered material properties by measuring the difference between the ground truth mean curvature and that of the recovered garment. We would like to mention that the curvature recovery is the process of material parameter recovery. However, the accuracy of recovered material parameters \mathcal{C} assessment involves a careful sensitivity study. For the purpose of this paper, we would keep our focus on the garment appearance recovery. As is shown in Table III, we are able to obtain more than **82%** accuracy for recovering local curvature.

Comparison: We compare our results with the multi-view reconstruction method, CMP-MVS [Jancosek and Pajdla 2011] together with the structure-from-motion framework [Wu 2011; Wu



Fig. 8. **Skirt recovery results.** We recover the highly occluded, folded skirts from the single-view images on the left [ModCloth 2015; AliExpress 2015] ©. The recovered human body meshes are shown in the middle overlaid on the original images. The recovered skirts are shown in the right.

Table II. **The accuracy of the recovered sizing parameters.**
The accuracy of the recovered sizing parameters of the t-shirt and the pants (in percentage).

TShirt Pants Scene						
Pose	a	a	b	b	c	c
Lighting	Mid-Day	Sunset	Mid-Day	Sunset	Mid-Day	Sunset
\mathcal{G}_{tshirt} Accuracy	90.2	88.3	89.8	88.1	88.3	86.3
\mathcal{G}_{pants} Accuracy	89.3	87.6	85.8	83.3	88.2	87.5

2013]. For a fair comparison, we apply smoothing [Taubin 1995]. Fig. 13 and Fig. 14 show the garment recovered using our method is clean and much closer to the original image.



Fig. 9. The input image (left) [Anthropologie 2015] © and the extracted human body part (middle) and recovered garment (right).

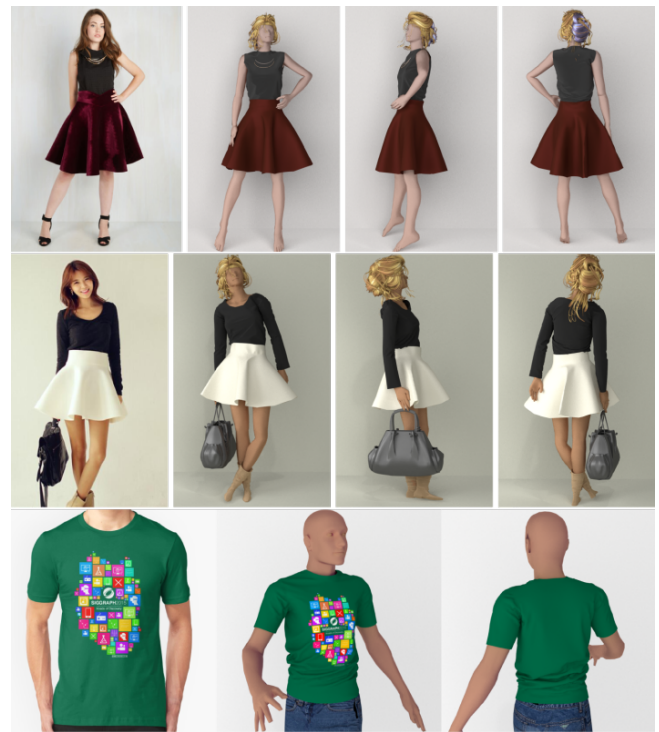


Fig. 10. For the first two rows, the input image (leftmost) [ModCloth 2015; AliExpress 2015; RedBubble 2015] ©. and recovered garment on the extracted human body. In the last row, the input image (leftmost) and the recovered garment on a twisted body (middle and right).

Without the depth information, an expert-designed 3D database, and a large manually labeled garment image database, our method achieves a fairly high accuracy compared with Chen et al. [2015] and higher quality compared with Zhou et al. [2013].



Fig. 11. **Image-based garment transfer results.** We dress the woman in (a) [FashionableShoes 2013; Boden 2015] © with the skirt we recovered from (b) [AliExpress 2015; ModCloth 2015] ©. (c) We simulate our recovered skirt with some wind motion to animate the retargeted skirt, as shown in (d). Another example of garment transfer is given in (e) - (h).



Fig. 12. **Synthetic evaluation scenes.** (a)-(c) fixed body shape with different poses. (d)-(e) fixed body shape with skirt of different material. (f)-(j) same scene setup as (a)-(e) but different lighting condition.

Table III. **The accuracy of recovered garment curvature.** The accuracy of the recovered garment local mean curvature of the skirt (in percentage).

T-Shirt Skirt Scene				
Material	Low Bending	Low Bending	High Bending	High Bending
Lighting	Mid-Day	Sunset	Mid-Day	Sunset
\mathcal{K}_{skirt} Accuracy	86.7	83.4	85.3	82.5



Fig. 13. **Comparison results.** (a) One frame of the video along with (b) the CMP-MVS results before and (c) after smoothing. (d) Our results using only one frame of the video.



Fig. 14. **Comparison results.** (a) One frame of the multi-view video along with (b) the CMP-MVS results before and (c) after smoothing. (d) Our results using only one frame of the video.

Performance: We run our method on a desktop with an Intel(R) Core(TM) i7 CPU, 3.20GHz. For each garment, our pipeline takes on average 4 to 6 hours. The garment parameter identification (Sec. 5) and joint material-pose optimization (Sec. 6.1) takes around 60% – 80% of the entire process. The preprocessing step (Sec. 4.2) takes around 20% – 30%. The performance depends largely on the complexity of the garment and on the image quality, and how much the garment occluded.

Limitations: The current implementation of our approach depends on two databases: the garment template database and human body database. The range of garments we can recover is limited by the available garment templates to some extent. Our parameter identification method can only generate garments that are “morphable” from the garment template, i.e. homeomorphic to the garment template. For example, since we use only one template for each garment type, we cannot yet model variations in some clothing details, e.g. multi-layered skirts, or collars on shirts. But for those garments that are not morphable from the template, our method can recover whichever version of the garment is closest to the true garment. With a more extensive set of templates we can begin to model more variations of styles and cuts, with richer garment details. Another limitation is the human body shape recovery. Our reduced human body shape is described by a set of semantic parameters \mathbf{z} . The representation of this set of semantic parameters is not enormous, though it is sufficient to include most of the common human body shapes, as shown in our images.

8. CONCLUSION AND FUTURE WORK

In this paper we present an algorithm for highly detailed garment recovery from a single-view image. Our approach recovers a 3D mesh of the garment together with the 2D design pattern, fine wrinkles and folds, and material parameters. The recovered garment can be re-targeted to other human bodies of different shapes, sizes, and poses for virtual try-on and character animation.

There are many possible future research directions. First of all, we plan to develop a parallelized implementation of our system on GPU or a many-core CPU for fast garment recovery. Both the underlying cloth simulator and the optimization process can be significantly accelerated. We also plan to extend our approach to enable fabric material transfer from video for interactive virtual try-on. Furthermore, we hope to explore possible perception metrics, similar in spirit to [Sigal et al. 2015], for evaluating our results.

REFERENCES

- AGARWAL, A. AND TRIGGS, B. 2006. Recovering 3d human pose from monocular images. *Pattern Analysis and Machine Intelligence, IEEE Transactions on* 28, 1, 44–58.
- ALIEXPRESS. 2015. <http://www.aliexpress.com>.
- ANGUELOV, D., SRINIVASAN, P., KOLLER, D., THRUN, S., RODGERS, J., AND DAVIS, J. 2005. Scape: shape completion and animation of people. In *ACM Transactions on Graphics (TOG)*. Vol. 24. ACM, 408–416.
- ANTHROPOLOGIE. 2015. <http://www.anthropologie.com>.
- BARAFF, D. AND WITKIN, A. 1998. Large steps in cloth simulation. In *Proceedings of the 25th annual conference on Computer graphics and interactive techniques*. ACM, 43–54.
- BÉRARD, P., BRADLEY, D., NITTI, M., BEELER, T., AND GROSS, M. 2014. High-quality capture of eyes. *ACM Transactions on Graphics (TOG)* 33, 6, 223.
- BERTHOUSOZ, F., GARG, A., KAUFMAN, D. M., GRINSPUN, E., AND AGRAWALA, M. 2013. Parsing sewing patterns into 3d garments. *ACM Transactions on Graphics (TOG)* 32, 4, 85.

- BODEN. 2015. <http://www.bodenusa.com>.
- BRIDSON, R., FEDKIW, R., AND ANDERSON, J. 2002. Robust treatment of collisions, contact and friction for cloth animation. In *ACM Transactions on Graphics (TOG)*. Vol. 21. ACM, 594–603.
- BRIDSON, R., MARINO, S., AND FEDKIW, R. 2003. Simulation of clothing with folds and wrinkles. In *Proceedings of the 2003 ACM SIGGRAPH/Eurographics symposium on Computer animation*. Eurographics Association, 28–36.
- BRONSTEIN, A. M., BRONSTEIN, M. M., AND KIMMEL, R. 2006. Efficient computation of isometry-invariant distances between surfaces. *SIAM Journal on Scientific Computing* 28, 5, 1812–1836.
- BRONSTEIN, A. M., BRONSTEIN, M. M., AND KIMMEL, R. 2008. *Numerical geometry of non-rigid shapes*. Springer Science & Business Media.
- BROUET, R., SHEFFER, A., BOISSIEUX, L., AND CANI, M.-P. 2012. Design preserving garment transfer. *ACM Trans. Graph.* 31, 4, 36.
- CAO, C., WENG, Y., LIN, S., AND ZHOU, K. 2013. 3d shape regression for real-time facial animation. *ACM Transactions on Graphics (TOG)* 32, 4, 41.
- CHAI, M., WANG, L., WENG, Y., YU, Y., GUO, B., AND ZHOU, K. 2012. Single-view hair modeling for portrait manipulation. *ACM Trans. Graph.* 31, 4 (July), 116:1–116:8.
- CHEN, X., GUO, Y., ZHOU, B., AND ZHAO, Q. 2013. Deformable model for estimating clothed and naked human shapes from a single image. *The Visual Computer* 29, 11, 1187–1196.
- CHEN, X., ZHOU, B., LU, F., WANG, L., BI, L., AND TAN, P. 2015. Garment modeling with a depth camera. *ACM Transactions on Graphics (TOG)* 34, 6, 203.
- CURTIS, S., TAMSTORF, R., AND MANOCHA, D. 2008. Fast collision detection for deformable models using representative-triangles. In *Proceedings of the 2008 symposium on Interactive 3D graphics and games*. ACM, 61–69.
- DECAUDIN, P., JULIUS, D., WITHER, J., BOISSIEUX, L., SHEFFER, A., AND CANI, M.-P. 2006. Virtual garments: A fully geometric approach for clothing design. In *Computer Graphics Forum*. Vol. 25. Wiley Online Library, 625–634.
- ENGLISH, E. AND BRIDSON, R. 2008. Animating developable surfaces using nonconforming elements. In *ACM Transactions on Graphics (TOG)*. Vol. 27. ACM, 66.
- FARABET, C., COUPRIE, C., NAJMAN, L., AND LECUN, Y. 2013. Learning hierarchical features for scene labeling. In *Pattern Analysis and Machine Intelligence*.
- FASHIONABLESHOES. 2013. <http://bestfashionableshoes.blogspot.com>.
- FASHIONUNITED. 2016. Global fashion industry statistics - international apparel.
- GOLDENTHAL, R., HARMON, D., FATTAL, R., BERCOVIER, M., AND GRINSPUN, E. 2007. Efficient simulation of inextensible cloth. *ACM Transactions on Graphics (TOG)* 26, 3, 49.
- GOVINDARAJU, N. K., KABUL, I., LIN, M. C., AND MANOCHA, D. 2007. Fast continuous collision detection among deformable models using graphics processors. *Computers & Graphics* 31, 1, 5–14.
- HASLER, N., ASBACH, M., ROSENHAHN, B., OHM, J.-R., AND SEIDEL, H.-P. 2006. Physically based tracking of cloth. In *Proc. of the International Workshop on Vision, Modeling, and Visualization, VMV*. 49–56.
- HASLER, N., STOLL, C., SUNKEL, M., ROSENHAHN, B., AND SEIDEL, H.-P. 2009. A statistical model of human pose and body shape. In *Computer Graphics Forum*. Vol. 28. Wiley Online Library, 337–346.
- HILLSWEDDINGDRESS. 2015. <http://hillsweddingdress.xyz>.
- HOUSE, D. H. AND BREEN, D. E. 2000. *Cloth modeling and animation*. AK Peters.
- JANCOSEK, M. AND PAJDLA, T. 2011. Multi-view reconstruction preserving weakly-supported surfaces. In *Computer Vision and Pattern Recognition (CVPR), 2011 IEEE Conference on*. 3121–3128.
- KAVAN, L., SLOAN, P.-P., AND O’SULLIVAN, C. 2010. Fast and efficient skinning of animated meshes. In *Computer Graphics Forum*. Vol. 29. Wiley Online Library, 327–336.
- KENNEDY, J. 2010. Particle swarm optimization. In *Encyclopedia of Machine Learning*. Springer, 760–766.
- LEVIN, A., LISCHINSKI, D., AND WEISS, Y. 2008. A closed-form solution to natural image matting. *Pattern Analysis and Machine Intelligence, IEEE Transactions on* 30, 2, 228–242.
- LI, H., LUO, L., VLASIC, D., PEERS, P., POPOVIĆ, J., PAULY, M., AND RUSINKIEWICZ, S. 2012. Temporally coherent completion of dynamic shapes. *ACM Transactions on Graphics* 31, 1 (January).
- LI, H., SUMNER, R. W., AND PAULY, M. 2008. Global correspondence optimization for non-rigid registration of depth scans. In *Computer graphics forum*. Vol. 27. Wiley Online Library, 1421–1430.
- LI, Y., SUN, J., TANG, C.-K., AND SHUM, H.-Y. 2004. Lazy snapping. In *ACM Transactions on Graphics (TOG)*. Vol. 23. ACM, 303–308.
- LINDNER, M. 2015. Global e-commerce sales set to grow 25% in 2015. <https://www.internetretailer.com/2015/07/29/global-e-commerce-set-grow-25-2015>.
- LIU, D. C. AND NOCEDAL, J. 1989. On the limited memory bfgs method for large scale optimization. *Mathematical programming* 45, 1-3, 503–528.
- LONG, J., SHELHAMER, E., AND DARRELL, T. 2015. Fully convolutional networks for semantic segmentation. *CVPR (to appear)*.
- MENG, Y., WANG, C. C., AND JIN, X. 2012. Flexible shape control for automatic resizing of apparel products. *Computer-Aided Design* 44, 1, 68–76.
- MODCLOTH. 2015. <http://www.modcloth.com>.
- MOESLUND, T. B., HILTON, A., AND KRÜGER, V. 2006. A survey of advances in vision-based human motion capture and analysis. *Computer vision and image understanding* 104, 2, 90–126.
- NAGANO, K., FYFFE, G., ALEXANDER, O., BARBIÇ, J., LI, H., GHOSH, A., AND DEBEVEC, P. 2015. Skin microstructure deformation with displacement map convolution. *ACM Trans. Graph.* 34, 4 (July), 109:1–109:10.
- NARAIN, R., SAMII, A., AND O’BRIEN, J. F. 2012. Adaptive anisotropic remeshing for cloth simulation. *ACM Transactions on Graphics (TOG)* 31, 6, 152.
- NG, H. N. AND GRIMSDALE, R. L. 1996. Computer graphics techniques for modeling cloth. *Computer Graphics and Applications, IEEE* 16, 5, 28–41.
- PINHEIRO, P. H. AND COLLOBERT, R. 2014. Recurrent convolutional neural networks for scene labeling. In *ICML*.
- POPA, T., ZHOU, Q., BRADLEY, D., KRAEVOY, V., FU, H., SHEFFER, A., AND HEIDRICH, W. 2009. Wrinkling captured garments using space-time data-driven deformation. In *Computer Graphics Forum*. Vol. 28. Wiley Online Library, 427–435.
- PROTOPSALTOU, D., LUIBLE, C., AREVALO, M., AND MAGNENAT-THALMANN, N. 2002. *A body and garment creation method for an Internet based virtual fitting room*. Springer.
- REDBUBBLE. 2015. <http://www.redbubble.com>.
- ROBSON, C., MAHARIK, R., SHEFFER, A., AND CARR, N. 2011. Context-aware garment modeling from sketches. *Computers & Graphics* 35, 3, 604–613.
- ROHMER, D., POPA, T., CANI, M.-P., HAHMANN, S., AND SHEFFER, A. 2010. Animation wrinkling: augmenting coarse cloth simulations with realistic-looking wrinkles. In *ACM Transactions on Graphics (TOG)*. Vol. 29. ACM, 157.

- SAACLOTHES. 2015. <http://www.saaclothes.com>.
- SCHOLZ, V. AND MAGNOR, M. 2006. Texture replacement of garments in monocular video sequences. In *Proceedings of the 17th Eurographics conference on Rendering Techniques*. Eurographics Association, 305–312.
- SCHOLZ, V., STICH, T., KECKEISEN, M., WACKER, M., AND MAGNOR, M. 2005. Garment motion capture using color-coded patterns. In *Computer Graphics Forum*. Vol. 24. Wiley Online Library, 439–447.
- SEO, H. AND MAGNENAT-THALMANN, N. 2003. An automatic modeling of human bodies from sizing parameters. In *Proceedings of the 2003 symposium on Interactive 3D graphics*. ACM, 19–26.
- SIGAL, L., MAHLER, M., DIAZ, S., MCINTOSH, K., CARTER, E., RICHARDS, T., AND HODGINS, J. 2015. A perceptual control space for garment simulation. *ACM Transactions on Graphics (TOG)* 34, 4, 117.
- SUMNER, R. W. AND POPOVIĆ, J. 2004. Deformation transfer for triangle meshes. *ACM Transactions on Graphics (TOG)* 23, 3, 399–405.
- TANG, M., CURTIS, S., YOON, S.-E., AND MANOCHA, D. 2009. Iccd: Interactive continuous collision detection between deformable models using connectivity-based culling. *Visualization and Computer Graphics, IEEE Transactions on* 15, 4, 544–557.
- TANIE, H., YAMANE, K., AND NAKAMURA, Y. 2005. High marker density motion capture by retroreflective mesh suit. In *Robotics and Automation, 2005. ICRA 2005. Proceedings of the 2005 IEEE International Conference on*. IEEE, 2884–2889.
- TAUBIN, G. 1995. A signal processing approach to fair surface design. In *Proceedings of the 22Nd Annual Conference on Computer Graphics and Interactive Techniques*. SIGGRAPH '95. ACM, New York, NY, USA, 351–358.
- TAYLOR, C. J. 2000. Reconstruction of articulated objects from point correspondences in a single uncalibrated image. In *Computer Vision and Pattern Recognition, 2000. Proceedings. IEEE Conference on*. Vol. 1. IEEE, 677–684.
- THOMASZEWSKI, B., PABST, S., AND STRASSER, W. 2009. Continuum-based strain limiting. In *Computer Graphics Forum*. Vol. 28. Wiley Online Library, 569–576.
- TURQUIN, E., WITHER, J., BOISSIEUX, L., CANI, M.-P., AND HUGHES, J. F. 2007. A sketch-based interface for clothing virtual characters. *IEEE Computer Graphics and Applications* 1, 72–81.
- VOLINO, P. AND MAGNENAT-THALMANN, N. 1999. Fast geometrical wrinkles on animated surfaces. In *Seventh International Conference in Central Europe on Computer Graphics and Visualization (Winter School on Computer Graphics)*.
- WANG, C. C., WANG, Y., AND YUEN, M. M. 2005. Design automation for customized apparel products. *Computer-Aided Design* 37, 7, 675–691.
- WANG, H., O'BRIEN, J., AND RAMAMOORTHI, R. 2010. Multi-resolution isotropic strain limiting. In *ACM Transactions on Graphics (TOG)*. Vol. 29. ACM, 156.
- WANG, H., O'BRIEN, J. F., AND RAMAMOORTHI, R. 2011. Data-driven elastic models for cloth: modeling and measurement. *ACM Transactions on Graphics (TOG)* 30, 4, 71.
- WEIL, J. 1986. The synthesis of cloth objects. *ACM Siggraph Computer Graphics* 20, 4, 49–54.
- WU, C. 2011. Visualsfm: A visual structure from motion system. URL: <http://homes.cs.washington.edu/~ccwu/vsfm> 9.
- WU, C. 2013. Towards linear-time incremental structure from motion. In *3D Vision - 3DV 2013, 2013 International Conference on*. 127–134.
- XIE, S. AND TU, Z. 2015. Holistically-nested edge detection. In *Proceedings of the IEEE International Conference on Computer Vision*. 1395–1403.
- YAMAGUCHI, K., KIAPOUR, M. H., AND BERG, T. 2013. Paper doll parsing: Retrieving similar styles to parse clothing items. In *Computer Vision (ICCV), 2013 IEEE International Conference on*. IEEE, 3519–3526.
- YANG, Y., YU, Y., ZHOU, Y., DU, S., DAVIS, J., AND YANG, R. 2014. Semantic parametric reshaping of human body models. In *3D Vision (3DV), 2014 2nd International Conference on*. Vol. 2. IEEE, 41–48.
- YOUNG, S., ADELSTEIN, B., AND ELLIS, S. 2007. Calculus of nonrigid surfaces for geometry and texture manipulation. *Visualization and Computer Graphics, IEEE Transactions on* 13, 5, 902–913.
- ZHAO, W., CHELLAPPA, R., PHILLIPS, P. J., AND ROSENFELD, A. 2003. Face recognition: A literature survey. *ACM computing surveys (CSUR)* 35, 4, 399–458.
- ZHOU, B., CHEN, X., FU, Q., GUO, K., AND TAN, P. 2013. Garment modeling from a single image. In *Computer Graphics Forum*. Vol. 32. Wiley Online Library, 85–91.
- ZHOU, S., FU, H., LIU, L., COHEN-OR, D., AND HAN, X. 2010. Parametric reshaping of human bodies in images. In *ACM Transactions on Graphics (TOG)*. Vol. 29. ACM, 126.